

## Some Surface and Catalytic Studies on Chromic-Oxide Gel

N. E. CROSS AND H. F. LEACH

*From the Department of Chemistry, University of Edinburgh, The King's Buildings, Edinburgh, EH9 3JJ, Scotland*

Received August 22, 1969; revised July 10, 1970

Three different samples of precipitated chromic oxide gel were prepared, and their surface and catalytic properties were studied.

The techniques of DTA, TGA, X-ray diffraction, and electron microscopy, together with adsorption measurements, have been used to provide information regarding the water content, porosity, and surface area of the samples. In particular, the manner in which these properties change as the pretreatment temperature is varied has been studied. The isomerization of *n*-but-1-ene, to *cis*-but-2-ene and *trans*-but-2-ene at 25°C, has been used as a test reaction to examine the manner in which the catalytic activity is dependent upon pretreatment temperature.

The initial *cis*-but-2-ene/*trans*-but-2-ene product ratio can give indications as to the type of reaction mechanism operative. The present work suggests that there are two different types of active sites on the chromic-oxide catalysts. At relatively low pretreatment temperatures, the reaction appears to proceed via a carbonium ion type of mechanism; and the sites responsible for such activity are believed to be associated with surface hydroxyl groups. At higher out-gassing temperatures the initial product ratio is greatly increased, and the reaction mechanism is best explained in terms of an allylic type of intermediate. It is suggested that the active sites responsible for this latter type of behavior are surface sites that are strained, such as would be produced by the removal of water from two adjacent hydroxyl groups.

### INTRODUCTION

Following the early work of Lazier and Vaughen (1) the catalytic and physical properties of chromic-oxide gels have been extensively examined. Oxide gels prepared by the slow addition, with stirring, of ammonia to a dilute solution of chromic nitrate exhibit catalytic activity. Burwell (2, 3) has shown that a similar catalyst can be prepared by simmering a solution of urea and chromic nitrate. The hydrolysis of the urea liberates the ammonia in a slow and uniform manner. The oxide has also been prepared by thermal decomposition  $\text{CrO}_3$  (4), and by low temperature decomposition of ammonium dichromate (5, 6).

In a study of reactions between hydrocarbons and deuterium over chromic-oxide

gels, Burwell *et al.* (2) indicated the importance of the activation temperature of the catalyst. In the isotopic exchange of alkanes, for example, significant activity was not observed until a pretreatment temperature of 300°C was used; maximum activity corresponded to an activation temperature of 470°C. Deren and co-workers (4) investigated the effect of pretreatment temperature upon the catalytic activity of several different preparations of chromic-oxide gel. Using the decomposition of hydrogen peroxide as their test reaction, maximum activity was observed after pretreatment of the catalyst in the temperature range 300–350°C.

There have been various reports (2, 7, 8, 9) concerning the structure of chromic-oxide gels, and attempts have been made to relate structural and physicochemical

changes to catalytic activity. Burwell has discussed briefly the effects of pore structure and other surface properties, and it was decided to study these aspects further. The isomerization of *n*-butenes, without skeletal rearrangement, was chosen as the test reaction. This was because a considerable amount of information has been gathered concerning this reaction, and also because both the rate of disappearance of the starting material and the product ratio can be measured. The latter quantity often provides a useful guide to the type of mechanism that is operative on the particular catalyst under study.

## EXPERIMENTAL

### *Materials*

Three gel samples were prepared in the following manner. For samples I and II, 0.5-*M* ammonia solution was added dropwise to a constantly stirred solution of chromic nitrate (0.5 *M*) maintained at a temperature of 78–82°C. The final pH values of the reaction mixture were 8.5 and 5.0, respectively. Sample III was prepared according to the method of Burwell and Taylor (3). A solution of urea and chromic nitrate was simmered at 100°C for several hours until abrupt precipitation of the gel occurred. The final pH of the solution was 5.4. All three samples were thoroughly washed with distilled water, then with acetone, and finally dried in an air oven at 60°C for 5 days.

The *n*-butenes (Matheson C.P. Grade) were further purified by repeated low temperature distillation. Before use, the purity was checked by gas chromatographic analysis.

### *Adsorption Studies*

Adsorption measurements were made with nitrogen as adsorbate at liquid nitrogen temperature using an apparatus based on the adsorption balance of McBain and Bakr (10). The samples were suspended in a silica bucket from a calibrated silica spring. They were then outgassed by evacuating the apparatus to a pressure of  $10^{-5}$  Torr and heating at the desired tempera-

ture for 12 hr. Changes in weight during the outgassing procedure and the subsequent adsorption were followed with a scale reading microscope (with a vernier scale) focussed on a fixed point on the suspension fiber.

Surface areas of less than 20 m<sup>2</sup>g<sup>-1</sup> were measured on a more sensitive apparatus in which the adsorption of krypton was followed using a volumetric arrangement (11).

### *Catalytic Studies*

Catalytic activity was studied by means of a static reaction system (100 ml) containing 0.1 g, before outgassing, of the hydrated catalyst. This was connected to a conventional gas-handling system on one side, and to a GLC column with flame ionization detector, recorder, and integrator on the other. Samples, consisting of approximately 2% of the gas phase, were periodically removed from the reaction vessel and swept through the column for analysis. The 4 meter column was packed with hexane-2,5-dione on 60/80 mesh Chromosorb P, and was operated at 0°C.

### *Physical Characterization*

Differential thermal analyses were carried out in still air on a Stanton Instrument against alumina as a standard, and with a rate of heating of 10°/min. Thermogravimetric analyses were made, again in still air, with a Stanton Mass Flow balance at a heating rate of 6°/min.

The X-ray measurements were made on a Philips Diffractometer operated at 40 kV with a 20 mA beam and a copper target.

The electron micrographs were taken with a Siemens Elmiskop 1A Electron Microscope. The samples were prepared by grinding a small amount with a mortar and pestle, and suspending the fine material in distilled cyclohexane. A drop of this suspension was then allowed to evaporate on to carbon-filmed specimen grids.

## RESULTS

### *Physical Characterization*

The differential thermal analyses (Fig. 1) of all three samples show essentially

the same features. The broad endotherm with a minimum of 200–220°C, and with an inflexion at about 160°C, has been attributed to loss of water by the highly hydrated gel leading to the formation of the trihydrate (12). A second endotherm, starting at about 240°C has been ascribed (4) to the decomposition of the trihydrate to monohydrate; in the present work it is difficult to distinguish this because of a superimposed exotherm arising from surface oxidation of the gel. However, the two distinct minima, at 220°C and 270°C, exhibited by gel II might possibly be attributed to the trihydrate and monohydrate species respectively. The very sharp exotherm occurring at 400–420°C results from the formation of crystalline  $\alpha$ -chromia via the well-known "glow" phenomenon.

Thermogravimetric analyses showed the three sample preparations to contain slightly differing amounts of water (II > III > I). A feature of all three analyses was an inflexion in the region corresponding to the trihydrate, which may be regarded as further evidence of the formation of this

compound as an intermediate during the dehydration process.

The X-ray analyses were used in a qualitative manner to determine the onset of crystallinity as a function of pretreatment temperature. All three samples displayed a diffraction pattern similar to that of crystalline  $\alpha$ -Cr<sub>2</sub>O<sub>3</sub> after pretreatment above 400°C. Higher pretreatment temperatures merely served to sharpen the diffraction lines.

#### Adsorption Studies

As seen in Figs. 2–4, the three gel samples exhibited markedly different surface characteristics, dependent upon the outgassing temperature used. With samples II and III, crystallization caused a substantial change in isotherm type; from type I to type IV, using the BDDT classification (14). With sample I, however, all three adsorption isotherms displayed a small hysteresis loop suggesting the existence of transitional pores (diameter in the range 30–200 Å), even at 430°C after some crystallization had occurred.

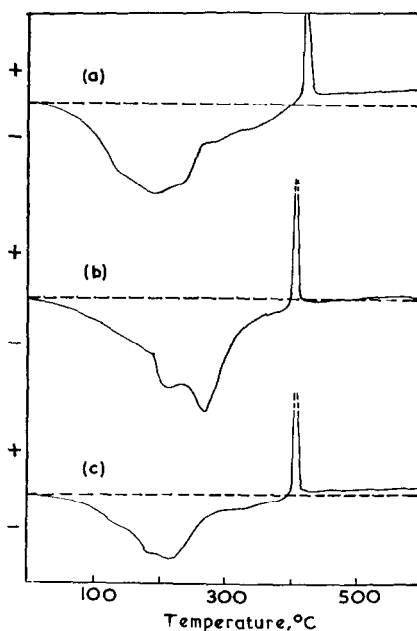


FIG. 1. Differential thermal analysis curves for the three chromic-oxide gel samples. (a) Cr<sub>2</sub>O<sub>3</sub>-I, (b) Cr<sub>2</sub>O<sub>3</sub>-II, and (c) Cr<sub>2</sub>O<sub>3</sub>-III.

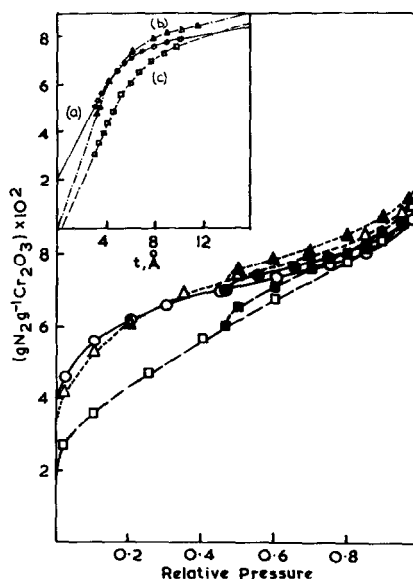


FIG. 2. Adsorption isotherms and  $t$ -plots (inset) for Cr<sub>2</sub>O<sub>3</sub>-I. (a) outgassed at 196°C (—○—), (b) outgassed at 364°C (---△---), and (c) outgassed at 431°C (---□---). The filled points refer to desorption.

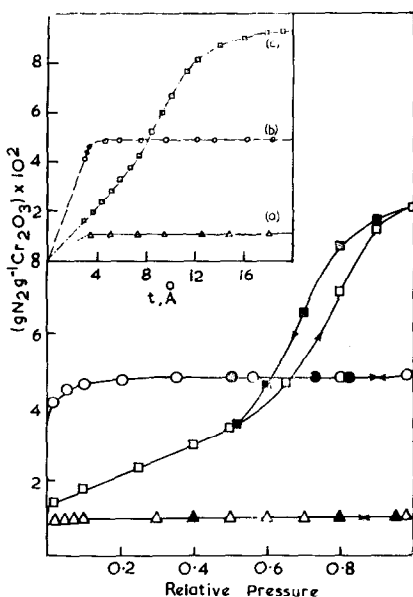


FIG. 3. Adsorption isotherms and  $t$ -plots (inset) for  $\text{Cr}_2\text{O}_3$ -II. (a) outgassed at  $270^\circ\text{C}$  (— $\Delta$ —), (b) outgassed at  $326^\circ\text{C}$  (— $\circ$ —), and (c) outgassed at  $431^\circ\text{C}$  (— $\square$ —). The filled points refer to desorption.

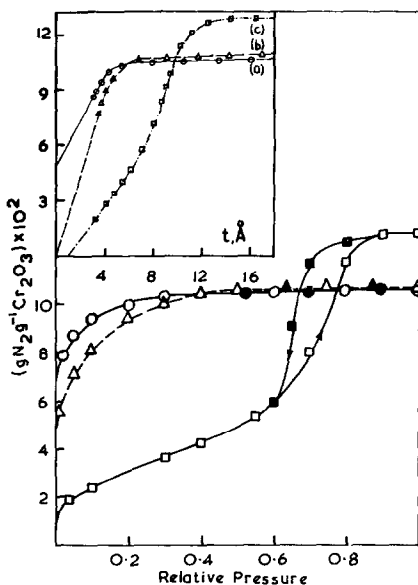


FIG. 4. Adsorption isotherms and  $t$ -plots (inset) for  $\text{Cr}_2\text{O}_3$ -III (a) outgassed at  $194^\circ\text{C}$  (— $\circ$ —), (b) outgassed at  $362^\circ\text{C}$  (--- $\Delta$ ---), and (c) outgassed at  $432^\circ\text{C}$  (— $\square$ —). The filled points refer to desorption.

The  $t$ -plots for sample I, derived from the isotherms and the data of de Boer and co-workers (13), indicated that a small but significant amount of the surface is associated with pores greater than micropore size. For example, with a sample of  $\text{Cr}_2\text{O}_3$ -I outgassed at  $364^\circ\text{C}$ ,  $14 \text{ m}^2\text{g}^{-1}$  are associated with transitional pores and external surface in a total B.E.T. surface area of  $177 \text{ m}^2\text{g}^{-1}$ . The intercept of the initial slope of the  $t$ -plot for the sample outgassed at  $196^\circ\text{C}$  is significantly above the origin, suggesting the presence of extremely small micropores.

The  $t$ -plot for the  $\text{Cr}_2\text{O}_3$ -II sample outgassed at  $270^\circ\text{C}$  suggests that the surface area is almost entirely associated with micropores (of diameter approximately equal to two molecular diameters of nitrogen). A line drawn from the origin to the first experimental point on the  $t$ -plot gave a value for the surface area of  $34 \text{ m}^2\text{g}^{-1}$ , comparable to the B.E.T. value of  $32 \text{ m}^2\text{g}^{-1}$ . The  $\text{Cr}_2\text{O}_3$ -II sample outgassed at  $326^\circ\text{C}$  showed similar characteristics but after the onset of crystallization (at  $431^\circ\text{C}$ ), the shape of the isotherm and the  $t$ -plot were altered. With the assumption that the pores are cylindrical, the maximum radius can be calculated at any given point on the isotherm from the Kelvin expression, i.e.,

$$r_{\max} = t + \frac{2\gamma V}{RT \ln P_0/P}$$

The  $t$ -plot showed that capillary condensation began at  $t = 6.5 \text{ \AA}$  (relative pressure of 0.50) which corresponded to a  $r_{\max}$  value of  $20 \text{ \AA}$ .

The adsorption data for  $\text{Cr}_2\text{O}_3$ -III gave a similar picture. The bulk of the surface for samples pretreated below  $400^\circ\text{C}$  was associated with micropores, whereas after outgassing at  $432^\circ\text{C}$  a hysteresis loop was observed. The onset of capillary condensation with this sample also occurred at  $t = 6.5 \text{ \AA}$ , corresponding to  $r_{\max} = 20 \text{ \AA}$ .

The variation of specific surface area with outgassing temperature is shown in Fig. 5. With all three gel samples the surface area increased to a maximum as water was removed. The somewhat different behavior of sample II could be explained by the difference in water content of this

sample. The absolute surface-area values (calculated by the B.E.T. procedure) for those isotherms which were of type I should be used with some caution.

The conditions during outgassing were found to be very important with respect to catalytic activity and surface properties. Samples of  $\text{Cr}_2\text{O}_3$ -III pretreated in air, oxygen or hydrogen, rather than vacuum, showed marked reductions in specific surface area; such reductions were accentuated if the gases contained water vapor. Heating in nitrogen or argon had no effect upon the properties of the oxide gel.

### Electron Micrographs

With very high magnifications it is possible to learn about the surface and its pore structure, and even to measure pore diameter (15). A less detailed analysis has been attempted here—the micrographs shown in Fig. 6 refer only to  $\text{Cr}_2\text{O}_3$ -I.

Sample (a), outgassed at  $364^\circ\text{C}$ , consisted of irregularly shaped particles of varying size. The centers of the larger particles were opaque to the electron beam, but the edges and smaller particles were transparent. On close examination, these transparent sections appear to contain a regular pattern of pores. Exact measurements of the pore diameter were not possible from the micrographs, even at the highest available magnification ( $\times 180000$ ),

due to the difficulty in determining a sharp line of contrast at the pore–solid interface. However, estimates tended to agree with the t-plot analysis in suggesting a pore diameter of  $< 20 \text{ \AA}$ . The three types of pores distinguished in the paper of Bowen and co-workers (16) for alumina seem to be present here:

- (i) large spaces between discrete particles, having no characteristic size or shape,
- (ii) smaller irregular holes in the particles, and
- (iii) an apparently regular array of uniform micropores.

Sample (b), outgassed at  $431^\circ\text{C}$ , showed irregularly shaped particles, largely in the form of microcrystallites, with more sharply defined edges. The larger particles retained the micropore structure but with pores of greater diameter. Such pores were less distinct and probably missing from the smaller crystallites. The surface area of this sample differed from that of (a) by only  $45 \text{ m}^2\text{g}^{-1}$ , and the general nature of the two isotherms were similar. The small, irregular, holes mentioned in connection with (a) were also found here, apparently in greater number.

Sample (c), outgassed at  $700^\circ$ , consisted of highly crystalline material with no micropore structure apparent. The particles were more angular and much larger, and they showed some evidence of buckling contours (black bands across the crystallites).

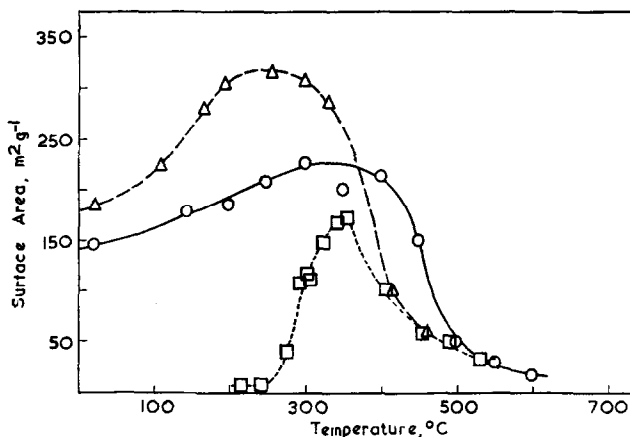


FIG. 5. Variation of specific surface area with outgassing temperature.  $\text{Cr}_2\text{O}_3$ -I (—○—),  $\text{Cr}_2\text{O}_3$ -II (---□---), and  $\text{Cr}_2\text{O}_3$ -III (---△---).

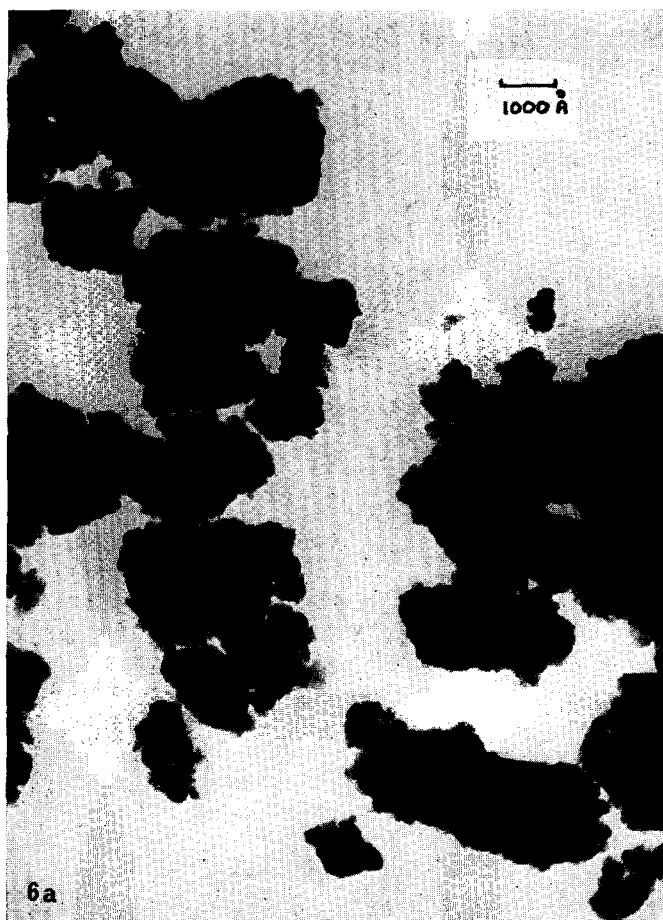


Fig. 6. Electron micrographs of  $\text{Cr}_2\text{O}_3$ -III (Magnification  $\times 120,000$ ) (a) after outgassing at  $364^\circ\text{C}$ , (b) after outgassing at  $431^\circ\text{C}$ , and (c) after outgassing at  $700^\circ\text{C}$ .

#### *Catalytic Activity for n-Butene Isomerization*

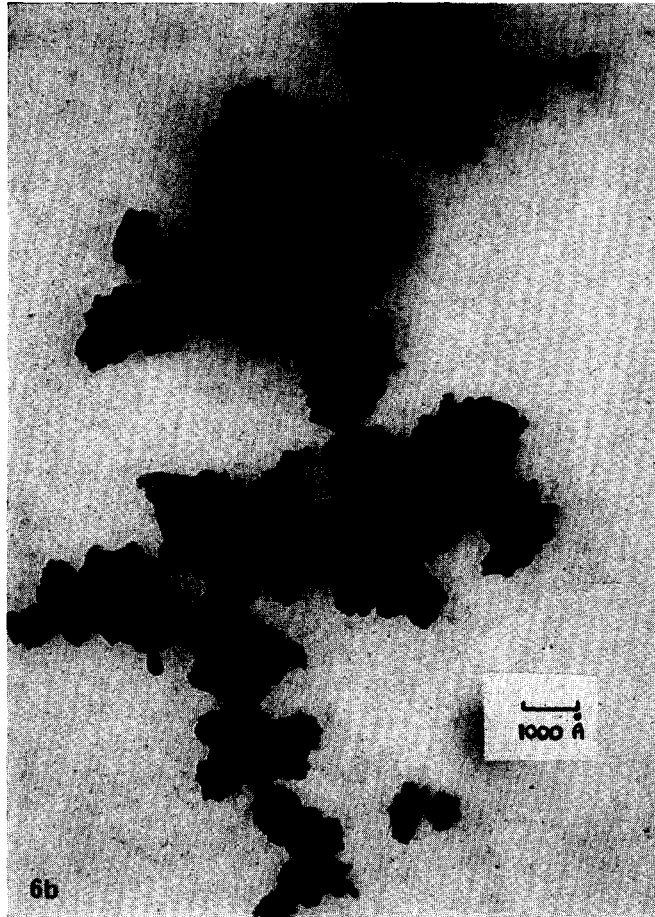
The reaction paths observed for the *n*-butene isomerization are illustrated by Fig. 7, which shows some results for  $\text{Cr}_2\text{O}_3$ -III. The catalytic results are summarized in Fig. 8 where the outgassing temperature of the chromic-oxide gels is correlated with (a) the rate of disappearance of but-1-ene at  $25^\circ\text{C}$ , and (b) the initial *cis*-but-2-ene/*trans*-but-2-ene product ratio.

The activity patterns for samples I and II were comparable with a maximum activity corresponding to a catalyst pretreatment temperature ca.  $550^\circ\text{C}$ , although sample II was considerably less active. With  $\text{Cr}_2\text{O}_3$ -III there was a small, but

distinct maximum corresponding to a pretreatment temperature of  $350^\circ\text{C}$ . Above this temperature the activity decreased only to rise rapidly at pretreatment temperatures greater than  $500^\circ\text{C}$ .

The feature of the initial product ratio data was the manner in which for all samples the ratio remained constant (at a value of 1-2) up to pretreatment temperatures of  $550$ - $600^\circ\text{C}$ , and then rose rapidly.

Experiments with *cis*-but-2-ene as initial reactant indicated that for all three samples the initial but-1-ene/*trans*-but-2-ene product ratio at low outgassing temperatures was 1, and this value rose slightly with increase in catalyst pretreatment temperature.



## DISCUSSION

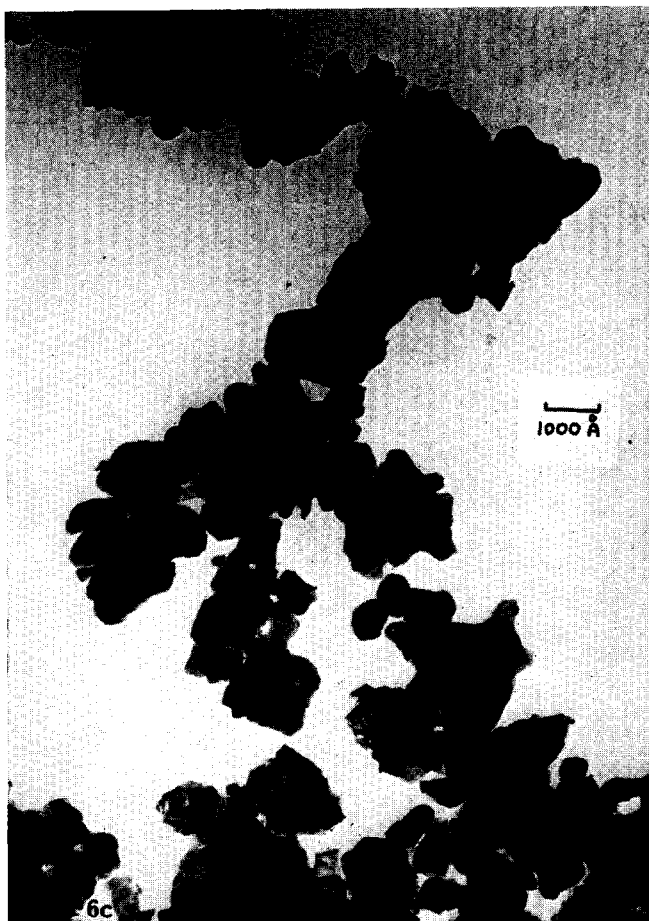
### *Surface Properties*

The changes in surface area exhibited by  $\text{Cr}_2\text{O}_3$ -I can be reasonably correlated with (a) the onset of crystallization as indicated by the X-ray measurements, and also with (b) the loss of water as illustrated by thermogravimetric analysis. The inability of the X-ray technique to detect the initial stages of crystallization would explain why the surface area began to decrease at temperatures somewhat below those at which crystallization was observed (400–410°C). The possible surface oxidation process (suggested by the DTA at 370°C) would also contribute to a loss in surface area prior to detectable crystallization.

The adsorption isotherms for  $\text{Cr}_2\text{O}_3$ -I

(Fig. 2) show that this sample contains both micropores and transitional pores. The changes observed as the outgassing temperature is increased are consistent with a process of pore widening as the water is removed; there is an increase in the number of transitional pores whereas the pores of very small diameter disappear. The electron micrographs (Fig. 6) lend some confirmation to such structural changes. The presence of micropores (diameter  $< 20 \text{ \AA}$ ) at 364°C, before crystallization, is clearly illustrated. This micropore structure is still in evidence at 431°C but has disappeared in the sample outgassed at 700°C when the crystallinity has become highly developed and the surface area very low.

The adsorption data for  $\text{Cr}_2\text{O}_3$ -II indicate that transitional pores only develop at temperatures above that required for



crystallization, and even then the total surface area was associated very much with the micropore structure. The DTA and TGA results indicate that this sample contained more water (strongly bound) than the other  $\text{Cr}_2\text{O}_3$  gels. The lack of development of appreciable surface area at outgassing temperatures below  $250^\circ\text{C}$  implies that at least 50% of the molecular water had to be removed before the internal micropore structure was accessible to nitrogen.

The structural differences between samples I and II could be attributed to the difference in pH of the final reaction mixture during the preparation—this could control the formation of larger particles. Carruthers (15) has suggested, however, that the conditions of mixing are more important than pH; while these conditions

were nominally the same for each preparation, it is possible that the stirring efficiencies were significantly different.

The  $\text{Cr}_2\text{O}_3$ -III sample has a pore structure consisting almost entirely of micropores at the lower outgassing temperatures, but the adsorption data indicate that a pore-widening process (with the formation of transitional pores) occurs at outgassing temperatures above  $400^\circ\text{C}$ .  $\text{Cr}_2\text{O}_3$ -III appears to be a more active and less stable solid than the other gels, as it exhibits the highest surface areas and has a maximum surface-area value at the relatively low pretreatment temperature of  $250^\circ\text{C}$ . This is consistent with the method of preparation (urea + chromic nitrate) which is known to produce a solid with uniform structure but with small particle size (2).



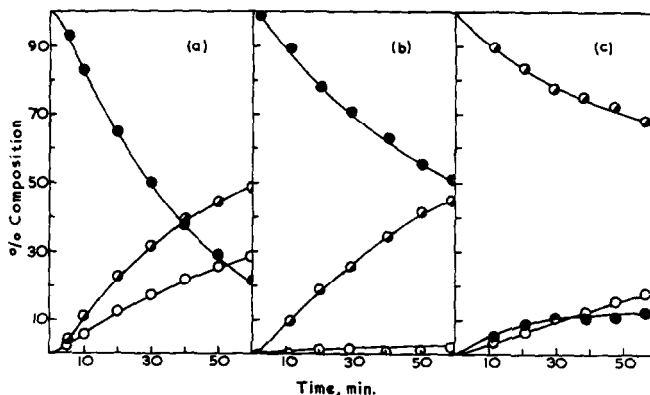


FIG. 7. Reaction paths for (a) but-1-ene at 25°C over Cr<sub>2</sub>O<sub>3</sub>-III, outgassed at 304°C, (b) but-1-ene at 25°C over Cr<sub>2</sub>O<sub>3</sub>-III, outgassed at 760°C, and (c) *cis*-but-2-ene at 50°C on Cr<sub>2</sub>O<sub>3</sub>-III, outgassed at 760°C. (—●— but-1-ene; —●— *cis*-but-2-ene; and —○— *trans*-but-2-ene.)

*Catalytic Activity*

It is well known that water, particularly molecular water, is an efficient poison for many reactions (17, 18), as it can block catalytically active sites. In this context the ability of the Cr<sub>2</sub>O<sub>3</sub>-I sample to exhibit appreciable catalytic activity only after approximately 75% of the water has been removed can be readily understood. The steady rise in activity with increase in pretreatment temperature up to 400°C is consistent with the increase in surface area and the decrease in amount of adsorbed water. Above this temperature the number of adsorbed water molecules becomes very small, and consequently the ratio of surface

sites to adsorbed water begins to rise sharply. The continual increase in activity per square meter of catalyst up to a pretreatment temperature of ca. 550°C, in spite of the specific surface area decrease at temperatures below this, can thus be explained.

At the high pretreatment temperatures the growth of well formed crystals is the predominant process—the pore structure has been effectively destroyed so surface-area changes will be relatively slow. There must therefore be several factors contributing to the sharp decline observed in the activity. Several authors have speculated on the nature of active sites in chromic-

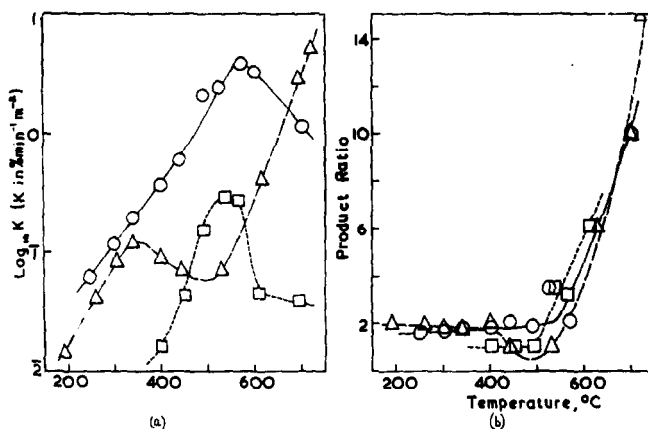


FIG. 8. (a) Activity pattern for disappearance of but-1-ene at 25°C as a function of outgassing temperature. (b) Variation in *cis*-but-2-ene/*trans*-but-2-ene product ratio with outgassing temperature. (○≡ Cr<sub>2</sub>O<sub>3</sub>-I, □≡ Cr<sub>2</sub>O<sub>3</sub>-II, and △≡ Cr<sub>2</sub>O<sub>3</sub>-III.)

oxide catalysts (2, 4, 19); the sites possibly arise from (a) reduction of surface  $\text{Cr}^{3+}$  to  $\text{Cr}^{2+}$ , (b) oxidation to  $\text{Cr}^{4+}$  and  $\text{Cr}^{6+}$ , (c) desorption of species such as water, or (d) the production of strained surface sites (as caused by the elimination of water from surface hydroxyl groups).

In the present investigation the product selectivity provides some indication of the nature of the sites active for the *n*-butene isomerization—particularly the very marked change that occurs after the point of maximum catalytic activity has been reached. At low pretreatment temperatures, the initial product ratios are consistent with a carbonium ion type of mechanism; the but-1-ene giving a *cis*-but-2-ene/*trans*-but-2-ene initial ratio close to 2, and *cis*-but-2-ene giving a *trans*-but-2-ene/but-1-ene initial ratio  $\geq 1$ . In such a mechanism both geometric and double-bond isomerization are envisaged as proceeding through a common intermediate, the *sec*-butyl carbonium ion. The active sites for such a reaction would be protonic, and we suggest that they are likely to be associated with surface hydroxyl groups which will become readily accessible after outgassing in the range 400–500°C.

With samples pretreated at temperatures above 550°C the predominant feature is a fast but-1-ene to *cis*-but-2-ene conversion, i.e., with but-1-ene giving an initial *cis*-but-2-ene/*trans*-but-2-ene ratio  $\gg 2$ , and *cis*-but-2-ene giving an initial *trans*-but-2-ene/but-1-ene ratio  $< 1$ . Such behavior is indicative of an allylic type of intermediate in which free rotation is hindered, and hence double-bond migration preferentially favored. Under these pretreatment conditions virtually all the surface hydroxyl groups will have been eliminated in the form of water, and strained surface sites are being formed. Consequently, it is attractive to link the observed change in behavior with such sites. Some support for this postulate is provided by the work of Burwell *et al.* (2), where the isomerization of hexene over an unsupported chromia catalyst (activated at 475°C) was believed to proceed via an allylic carbanion mechanism.

Ogasawana and Cvetanovic (20) suggested that *n*-butene isomerization over

alumina involved two different mechanisms simultaneously; the *cis-trans* geometrical isomerization occurring via a carbonium ion mechanism, and the double-bond shift via an allylic intermediate or via the concerted hydrogen-switch mechanism (21). In the present work it would thus appear that a process of deactivation of the carboniogenic sites and generation of the allylic type sites would explain the observed product selectivity changes with increasing pretreatment temperature.

The catalytic activity patterns for the  $\text{Cr}_2\text{O}_3$ -II and  $\text{Cr}_2\text{O}_3$ -III samples can be explained in terms of the picture developed for the  $\text{Cr}_2\text{O}_3$ -I gel. The lower overall activity of the  $\text{Cr}_2\text{O}_3$ -II sample could be attributed to the presence of more strongly bound water. The two distinct regions of catalytic activity displayed by the  $\text{Cr}_2\text{O}_3$ -III sample suggest that in this particular case virtually all the carboniogenic activity is lost before sites become activated for the allylic double-bond shift mechanism.

Chen and co-workers (22) concluded that their results for *n*-butene isomerization at 325°C over a chromia-alumina catalyst were best explained in terms of the parallel mechanisms proposed by Carra and Ragaini (23). These were invoked to explain the isomerization over metal catalysts: they involve (i) a carbonium ion intermediate (associated with two surface sites) which yields only *cis*-but-2-ene on desorption, and (ii) an allylic radical which is not stereoselective. The results of the present study are not satisfactorily explained in terms of such a reaction scheme.

Burwell and co-workers (7) have suggested that the narrow microporous structure found in amorphous chromic-oxide gels may result in special catalytic behavior. The present investigation with the three different gel preparations certainly illustrates further that the amount of surface available, and its form, play a vital role in the type of catalytic activity displayed.

#### ACKNOWLEDGMENTS

Acknowledgment is made to the S.R.C. for financial support for N.E.C. The authors are grateful to Mr. T. Baird of Glasgow University,

who prepared the electron micrographs, and also to Dr. S. C. Bevan of Brunel University, who performed some of the differential thermal analyses.

## REFERENCES

1. LAZIER, W. A., AND VAUGHEN, J. V., *J. Amer. Chem. Soc.* **54**, 3080 (1932).
2. BURWELL, R. L., LITTLEWOOD, A. B., CARDEW, M., PASS, G., AND STODDART, C. T. H., *J. Amer. Chem. Soc.* **82**, 6272 (1960).
3. BURWELL, R. L., AND TAYLOR, H. S., *J. Amer. Chem. Soc.* **58**, 697 (1936).
4. DEREN, J., HABER, J., PODGORECKA, A., AND BURZYK, J., *J. Catal.* **2**, 161, (1963).
5. BURZYK, J., DEREN, J., AND HABER, J., *Int. Symp. Reactiv. Solids, 5th Munich* (1964).
6. RAO, S. R., SANDLE, N. K., AND RAMAKRISHNA, V., *Ind. J. Chem.* **6**, 36 (1968).
7. BURWELL, R. L., TAYLOR, K. C., AND HALLER, G. L., *J. Phys. Chem.* **71**, 4580 (1967).
8. BHATTACHARYYA, S. K., RAMACHANDRAN, V. S., AND GHOSH, J. C., *Advan. Catal. Relat. Subj.* **9**, 114 (1957).
9. SING, K. S. W., CARRUTHERS, J. D., AND FENERTY, J., *Nature* **213**, 66 (1967).
10. MCBAIN, J. W., AND BAKR, A. M., *J. Amer. Chem. Soc.* **48**, 690 (1926).
11. INGLIS, H. S., PhD Thesis, Edinburgh, 1966.
12. HANTZSCH, A., AND TORKE, E., *Z. Anorg. Allg. Chem.* **209**, 60 (1932).
13. LIPPENS, B. C., LINSEN, B. G., AND DE BOER, J. H., *J. Catal.* **3**, 32 (1964).
14. BRUNAUER, S., DEMING, L. S., DEMING, W. E., AND TELLER, E., *J. Amer. Chem. Soc.* **62**, 1723 (1940).
15. CARRUTHERS, J. D., PhD Thesis, Brunel, 1968.
16. BOWEN, J. H., BOWREY, R., AND MALIN, A. S., *J. Catal.* **7**, 209 (1967).
17. SALLEY, D. J., FEHRER, H., AND TAYLOR, H. S., *J. Amer. Chem. Soc.* **63**, 1131 (1941).
18. WELLER, S. W., AND VOLTZ, S. E., *J. Amer. Chem. Soc.* **76**, 4695 (1954).
19. WELLER, S. W., AND VOLTZ, S. E., *Z. Phys. Chem.* **5**, 100 (1955).
20. OGASAWANA, S., AND CVETANOVIC, R. J., *J. Catal.* **2**, 45 (1963).
21. TURKEVICH, J., AND SMITH, R. K., *J. Chem. Phys.* **16**, 466 (1948).
22. CHEN, H. C., HUDGINS, R. R., AND SILVESTON, P. L., *Can. J. Chem.* **47**, 323 (1969).
23. CARRA, S., AND RAGAINI, V., *J. Catal.* **10**, 230 (1968).